ВІСНИК ЛЬВІВ. УН-ТУ *VISNYK LVIV UNIV.*
Серія фізична. 2007. Вип.40. С.219-231 *Ser.Physic. 2007. N40. P.219-231*

PACS number(s): 72.20.Jv, 72.80.Ng

THERMALLY STIMULATED CURRENTS IN DISORDERED SOLIDS AT STEP HEATING

W. Tomaszewicz[1], P. Grygiel

Department of Physics of Electronic Phenomena
Gdansk University of Technology
G. Narutowicza 11/12, PL-80952 Gdansk, Poland
[1]e-mail: wtomasze@sunrise.pg.gda.pl

In the paper, thermally stimulated currents (TSCs) in disordered solids due to step sample heating are investigated theoretically. The Gobrecht-Hofmann method of TSC analysis is extended to the case of meaningful carrier retrapping. Two kinds of experiments concerning TSCs measured in samples with either coplanar or sandwich electrodes are considered. The main factor limiting TSC is then, respectively, either carrier recombination assumed to be monomolecular or bimolecular, or carrier neutralization on the collecting electrode. In all the cases simple formulas are given, which make possible to determine the energetic distribution of traps from the dependence of released charge on activation energy of the initial TSC rise during sequential heating cycles. Their accuracy is estimated by analysing TSC curves, calculated numerically for exponential trap distribution.

Key words: thermally stimulated currents, step heating, carrier trapping, carrier recombination, multiple-trapping model, amorphous solids.

The TSC experiments consist in photogenerating of excess charge carriers in a sample cooled to a low temperature, and registering current flowing in measuring circuit in course of subsequent sample heating. The resulting TSC is due to carrier release from trapping states of investigated solid and yields information about their energy distribution and/or density. Two kinds of experiments can be distinguished: (1) Sample with coplanar electrodes is illuminated by weakly absorbed light. TSC is then determined by carrier trapping/detrapping and recombination ('TSC recombination peak', TSCRP). (2) Sample having sandwich electrodes is excited by strongly absorbed light. In this case TSC is due to one-sign carrier transport and neutralization on collecting electrode ('TSC transport peak', TSCTP).

In majority of TSC measurements the sample is heated with a constant rate after the end of excitation. Sometimes, more complex heating schemes are utilized. One of them is the step heating, when the sample is linearly heated to some temperature, rapidly cooled to initial temperature, heated to higher temperature, and so on (cf. Fig. 1). Such TSC measurements were performed for many disordered solids, e.g., amorphous hydrogenated silicon [1–3] and photoconducting polymers [4–8]. However, the

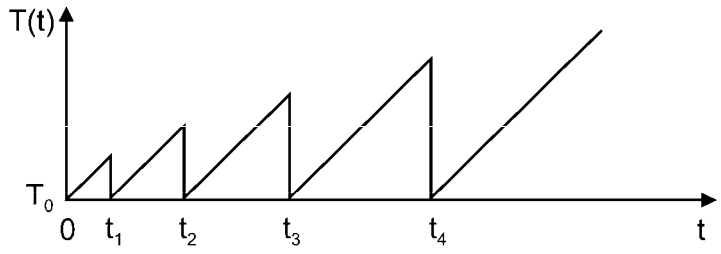

Fig. 1. Time dependence of the sample temperature in the case of step heating

corresponding theory is still incomplete. In principle all the methods of analysis of TSCs registered at fractional heating (see [9], p. 172–177) should be also applicable to the case of step heating. In these methods, however, carrier retrapping is ignored, which limits their usefulness and may yield incorrect results. More detailed descriptions of TSCs at step heating, including carrier retrapping, concerned mainly the initial TSC rise [10–13].

In this paper, we present the extension of the Gobrecht-Hofmann method to the case of meaningful carrier retrapping. The method was primarily used for analysis of thermally stimulated luminescence at fractional heating [14], and subsequently adopted for analysis of thermostimulated currents, e.g., [7–9]. It consists in determination of the energetic distribution of traps from the dependence of released charge on activation energy of the initial TSC rise, during sequential heating cycles. Both TSCRPs, corresponding to monomolecular and bimolecular carrier recombination, as well as TSCTPs are considered. The analytical results are compared with the numerical ones, obtained for exponential trap distribution.

The present study is based on earlier descriptions of TSCRPs [15] and TSCTPs [16] in disordered materials. Although they concerned linear sample heating, the obtained results should apply after slight changes for other heating schemes. The validity of the multiple-trapping model and the existence of continuous distribution of trapping states in the energy gap were assumed. The main simplifying assumptions were: (1) negligibly small trap occupancy, and (2) strongly non-equilibrium distribution of trapped carriers. The second assumption is adequate, if the trap density varies slowly in energy gap compared to the Boltzmann factor.

According to [15-16], the intensities of TSCRP and TSCTP can be expressed as

$$I(t) = \frac{\mathrm{d}Q\left[\varepsilon_0(t)\right]}{\mathrm{d}t}. \tag{1}$$

Here, t is the time variable, Q(...) is the collected charge, and $\varepsilon_0(t)$ is the demarcation energy level, defined implicitly by the equation

$$\int_0^t \frac{\mathrm{d}t'}{\tau_r\left[\varepsilon_0(t), t'\right]} = 1, \tag{2}$$

where

$$\tau_r(\varepsilon, t) = \frac{1}{\nu_0} \exp\left[\frac{\varepsilon}{kT(t)}\right] \tag{3}$$

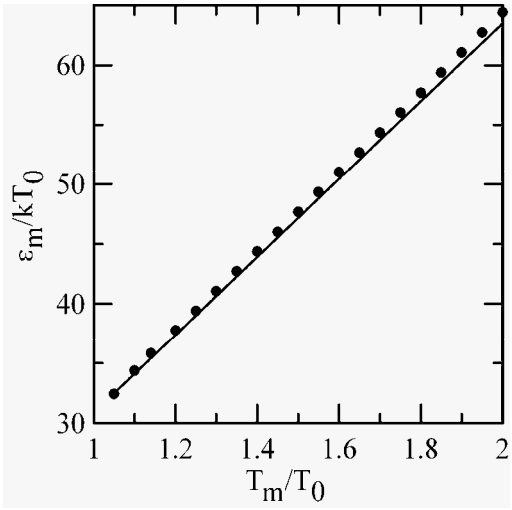

Fig. 2. Dependence of the demarcation energy on the maximum temperature of preceding heating cycle, calculated from Eqs. (2)–(4) (points) for 20 heating cycles, and from approximate Eqs. (5)–(6) (solid line). $\nu_0 T_0/\beta = 10^{15}$, $T_0 = 100$ K

is the mean carrier dwell-time in the traps of depth ε, measured from the edge of allowed band (ν_0 – the frequency factor, k – the Boltzmann constant and T(t) – the sample temperature).

The time dependence of demarcation energy $\varepsilon_0(t)$ in the case of step heating,

$$T(t) = T_0 + \beta(t - t_{m-1}), \quad t_{m-1} < t \le t_m, \quad m = 1,2,3,\ldots(t_0 = 0) \tag{4}$$

(T_0 – the initial temperature, β - the heating rate), was investigated in [12]. At the onset of the (m+1)th heating cycle $\varepsilon_0(t) \cong \varepsilon_m$ and $d\varepsilon_0(t)/dt \propto \exp[-\varepsilon_m/kT(t)]$, where the energy

$$\varepsilon_m \cong k\left(c^* T_m - T^*\right), \tag{5}$$

with

$$c^* = 0{,}967 \ln\left(46\,\mathrm{K} \cdot \nu_0/\beta\right), \quad T^* = 180\,\mathrm{K}, \tag{6}$$

and $T_m = T(t_m)$.The accuracy of Eqs. (5)-(6) is illustrated by Fig. 2. From Eq. (1) it follows that the initial TSC increase has thermally activated character,

$$I(t) \propto \exp\left[-\varepsilon_m / kT(t)\right], \quad t \cong t_m. \tag{7}$$

Therefore, the TSC measurements at step heating enable us to determine the approximate values of demarcation energy $\varepsilon_m = \varepsilon_0(t_m)$ and of frequency factor ν_0.

The formulas for the collected charge $Q[\varepsilon_0(t)]$ were derived in [15–16]. The charge expresses in terms of the function

$$\Phi(t) \cong C_t \int_{\varepsilon_0(t)}^{\varepsilon_t} N_t(\varepsilon)\,d\varepsilon, \quad \varepsilon_t^0 \le \varepsilon_0(t) \le \varepsilon_t, \tag{8}$$

where C_t is the carrier capture coefficient, $N_t(\varepsilon)$ is the trap density per energy unit, and ε_t^0 and ε_t are the trap distribution limits. The Φ(t) function determines the probability

that the carrier is captured in time unit in the trap of depth $\varepsilon \geq \varepsilon_0(t)$ and stays in the trap up to time t. In what follows, we shall present the formulas for $Q(\varepsilon_m)$ and the resulting formulas which make possible to determine the trap density. For simplicity, we shall write here ε instead of ε_m.

TSCRP, *monomolecular recombination*

The collected charge is given by

$$Q(\varepsilon) = \frac{Q_\infty}{\tau_R \Phi(\varepsilon) + 1} \tag{9}$$

(cf. [15]), where Q_∞ is the total collected charge corresponding to the area under TSC curve and τ_R is the mean time of carrier recombination. Making use of Eq. (8) one obtains:

$$\tau_R C_t \int_{\varepsilon}^{\varepsilon_t} N_t(\varepsilon')\,\mathrm{d}\varepsilon' = \frac{Q_\infty}{Q(\varepsilon)} - 1. \tag{10}$$

If $Q(\varepsilon) << Q_\infty$, Eq. (10) simplifies to

$$\tau_R C_t \int_{\varepsilon}^{\varepsilon_t} N_t(\varepsilon')\,\mathrm{d}\varepsilon' \cong \frac{Q_\infty}{Q(\varepsilon)}. \tag{11}$$

Differentiating Eq. (10) over energy one gets:

$$\tau_R C_t N_t(\varepsilon) = \frac{Q_\infty}{Q^2(\varepsilon)} \cdot \frac{\mathrm{d}Q(\varepsilon)}{\mathrm{d}\varepsilon}. \tag{12}$$

When $Q(\varepsilon) \cong Q_\infty$, Eq. (12) can be approximated by

$$\tau_R C_t N_t(\varepsilon) \cong \frac{1}{Q_\infty} \cdot \frac{\mathrm{d}Q(\varepsilon)}{\mathrm{d}\varepsilon}. \tag{13}$$

TSCRP, bimolecular recombination

The $\Phi(\varepsilon)$ function is interrelated with the collected charge by the formula

$$\Phi(\varepsilon) = \frac{C_R n_0 Q_R}{Q(\varepsilon)} \exp\left[-\frac{Q(\varepsilon)}{Q_R} \right] \tag{14}$$

(see [15]). Here, C_R is the carrier recombination coefficient, n_0 is the initial density of generated carriers, and the charge

$$Q_R = \frac{e\mu_0 ES}{C_R} \tag{15}$$

(with e – the elementary charge, μ_0 - the free carrier mobility, E – the electric field strength, and S – the sample cross-section area, perpendicular to the carrier flow direction). From Eqs. (8) and (14) it follows that

$$\frac{C_t}{C_R n_0} \int_{\varepsilon}^{\varepsilon_t} N_t(\varepsilon')\,\mathrm{d}\varepsilon' = \frac{Q_R}{Q(\varepsilon)} \exp\left[-\frac{Q(\varepsilon)}{Q_R} \right]. \tag{16}$$

When $Q(\varepsilon) << Q_R$, Eq. (16) may be simplified to

$$\frac{C_t}{C_R n_0} \int_{\varepsilon}^{\varepsilon_t} N_t(\varepsilon')\,\mathrm{d}\varepsilon' \cong \frac{Q_R}{Q(\varepsilon)}. \tag{17}$$

By differentiation of Eq. (16) one gets the formula

$$\frac{C_t}{C_R n_0} N_t(\varepsilon) = \frac{1}{Q(\varepsilon)}\left[1+\frac{Q_R}{Q(\varepsilon)}\right]\exp\left[-\frac{Q(\varepsilon)}{Q_R}\right]\frac{\mathrm{d}Q(\varepsilon)}{\mathrm{d}\varepsilon}, \tag{18}$$

which for $Q(\varepsilon) << Q_R$ simplifies to

$$\frac{C_t}{C_R n_0} N_t(\varepsilon) \cong \frac{Q_R}{Q^2(\varepsilon)} \cdot \frac{\mathrm{d}Q(\varepsilon)}{\mathrm{d}\varepsilon}. \tag{19}$$

TSCTP

The collected charge is expressed by

$$Q(\varepsilon) = Q_\infty \frac{1-\exp\left[-\tau_0 \Phi(\varepsilon)\right]}{\tau_0 \Phi(\varepsilon)} \tag{20}$$

[16], where

$$\tau_0 = \frac{d}{\mu_0 E} \tag{21}$$

is the free carrier time-of-flight (d – sample thickness). According to Eqs. (8) and (20)

$$\tau_0 C_t \int_{\varepsilon}^{\varepsilon_t} N_t(\varepsilon')\mathrm{d}\varepsilon' = F_1\left[\frac{Q(\varepsilon)}{Q_\infty}\right], \tag{22}$$

where the function $y = F_1(x)$ $(0 \le x \le 1)$ is defined as inverse of the function

$$x = \frac{1-\exp(-y)}{y}. \tag{23}$$

The properties of the $F_1(...)$ function are discussed in Appendix. According to them, for $Q(\varepsilon) << Q_\infty$ Eq. (22) can by approximated by

$$\tau_0 C_t \int_{\varepsilon}^{\varepsilon_t} N_t(\varepsilon')\mathrm{d}\varepsilon' \cong \frac{Q_\infty}{Q(\varepsilon)}, \tag{24}$$

and for $Q(\varepsilon) \cong Q_\infty$ by

$$\tau_0 C_t \int_{\varepsilon}^{\varepsilon_t} N_t(\varepsilon')\mathrm{d}\varepsilon' \cong 2\left[1-\frac{Q(\varepsilon)}{Q_\infty}\right]. \tag{25}$$

Differentiation of Eq. (22) gives the formula

$$\tau_0 C_t N_t(\varepsilon) = \frac{1}{Q_\infty} F_2\left[\frac{Q(\varepsilon)}{Q_\infty}\right]\frac{\mathrm{d}Q(\varepsilon)}{\mathrm{d}\varepsilon}, \tag{26}$$

where the function

$$F_2(x) = -\frac{\mathrm{d}F_1(x)}{\mathrm{d}x}. \tag{27}$$

The behaviour of the $F_2(...)$ function is also considered in Appendix. From Eq. (26) the following approximate formulas result. For $Q(\varepsilon) << Q_\infty$

$$\tau_0 C_t N_t(\varepsilon) \cong \frac{Q_\infty}{Q^2(\varepsilon)} \cdot \frac{\mathrm{d}Q(\varepsilon)}{\mathrm{d}\varepsilon}, \tag{28}$$

and for $Q(\varepsilon) \cong Q_\infty$

$$\tau_0 C_t N_t(\varepsilon) \cong \frac{2}{Q_\infty} \cdot \frac{\mathrm{d}Q(\varepsilon)}{\mathrm{d}\varepsilon}. \tag{29}$$

One should indicate some similarities between formulas describing TSCRP at monomolecular and bimolecular recombination and TSCTP. Let us consider first initial behaviour of TSCs, when $Q(\varepsilon) << Q_\infty$ or $Q(\varepsilon) << Q_R$. According to [15-16] the following relationships hold:

$$Q_\infty = I_0 \tau_R \tag{30}$$

(TSCRP, monomolecular recombination),

$$Q_R = \frac{I_0}{C_R n_0} \tag{31}$$

(TSCRP, bimolecular recombination), and

$$Q_\infty = I_0 \tau_0 \tag{32}$$

(TSCTP), where

$$I_0 = e n_0 \mu_0 E S \tag{33}$$

is the current intensity, corresponding to the motion of all generated carriers in the allowed band. Thus, Eqs. (11), (17) and (24) may be rewritten as

$$\frac{C_t}{I_0} \int_{\varepsilon}^{\varepsilon_t} N_t(\varepsilon') \mathrm{d}\varepsilon' \cong \frac{1}{Q(\varepsilon)}, \tag{34}$$

and Eqs. (12), (19) and (28) as

$$\frac{C_t}{I_0} N_t(\varepsilon) \cong \frac{1}{Q^2(\varepsilon)} \cdot \frac{\mathrm{d}Q(\varepsilon)}{\mathrm{d}\varepsilon}. \tag{35}$$

These identities result from the fact that initial increase of TSC is independent of carrier recombination or neutralization at collecting electrode.

Let us consider now final behaviour of TSCRPs at monomolecular recombination and TSCTPs, when $Q(\varepsilon) \cong Q_\infty$. Then, from Eqs. (13) and (29) the following relationship results:

$$N_t(\varepsilon) \propto \frac{\mathrm{d}Q(\varepsilon)}{\mathrm{d}\varepsilon}. \tag{36}$$

The relationship implies that carrier retrapping does not influence the final decay of TSC (cf. [15-16]). Since the Gobrecht-Hofmann method ignores the carrier retrapping, one can conclude that the method applies solely to TSCRPs at monomolecular recombination and TSCTPs in the final temperature region.

The given formulas enable us to determine the energetic trap distribution with accuracy to multiplicative coefficients from the TSC courses measured in entire temperature region. In the case of TSCRPs the kinetics of carrier recombination must be known; for bimolecular recombination the knowledge of the value of C_t/μ_0 is also necessary (see Eq. (15)). This value may be determined from the dependence of TSCRP on the initial carrier density, n_0.

As already indicated, from the TSC measurements the dependence of the collected charge after m heating cycles on the corresponding demarcation energy, $Q(\varepsilon_m)$, can be determined. Two methods of calculating the trap density can be proposed:

(A) The total trap density in the energy region $\varepsilon_m \le \varepsilon \le \varepsilon_t$ may be found directly from Eqs. (10), (16) and (22) or corresponding approximate equations. The trap density $N_t(\varepsilon_m)$ can be next calculated by numerical differentiation of the total trap density.

(B) The trap density $N_t(\varepsilon_m)$ may be calculated from Eqs. (12), (18) and (26). In these equations, the charge derivatives must be approximated by finite differences, viz.

$$\left.\frac{\mathrm{d}Q(\varepsilon)}{\mathrm{d}\varepsilon}\right|_{\varepsilon=\varepsilon_m} \cong \frac{\Delta Q_m}{\Delta\varepsilon_m}, \tag{37}$$

where

$$\Delta Q_m = Q(\varepsilon_m) - Q(\varepsilon_{m-1}), \quad \Delta\varepsilon_m = \varepsilon_m - \varepsilon_{m-1}. \tag{38}$$

One can expect that both methods have similar accuracy.

In order to check the accuracy of given formulas we performed the numerical calculations of TSCs and the collected charge at step sample heating. In the cases of TSCRPs at monomolecular recombination and TSCTPs the Monte Carlo method has been utilized, whereas in the case of TSCRPs at bimolecular recombination the finite-differences method has been used. The numerical methods were similar to those described in our earlier papers, e.g., [16-18]. As the model trap distribution the exponential one,

$$N_t(\varepsilon) = \frac{N_{tot}}{kT_C}\exp\left(-\frac{\varepsilon-\varepsilon_t^0}{kT_C}\right), \quad \varepsilon_t = \infty, \tag{39}$$

has been chosen. Here, N_{tot} denotes the total trap density, and the characteristic temperature T_C determines the rate of trap density decay in the energy gap.

In Fig. 3–8 the numerical and analytical results (marked respectively by points and continuous lines) are compared. Fig. 3 *a*, *b* show the TSCRP curves at monomolecular recombination in semi-logarithmic scale plotted versus T_0/T for two values of the characteristic temperature, $T_C/T_0=3$ and $T_C/T_0=5$, respectively. The calculation parameter $\tau_t = 1/C_tN_{tot}$. The numbers on the plots refer to given heating cycles. Only the results corresponding to even cycles are shown. Fig. 4 *a*, *b* present in semi-logarithmic scale the derivative of collected charge over energy and the collected charge, respectively, for the $T_C/T_0=5$ value. Figs. 5–6 and 7–8 show analogous results, concerning respectively to TSCRPs at bimolecular recombination and TSCTPs.

As can be seen, there exists rather good agreement between numerical and analytical results. The initial TSC rise is somewhat slower than predicted by Eq. (7). This may cause some error in determination of demarcation energy ε_m, probably not exceeding 10%. As expected, the accuracy of analytical results improves with the increasing value of characteristic temperature T_C. It should be stressed that the courses of

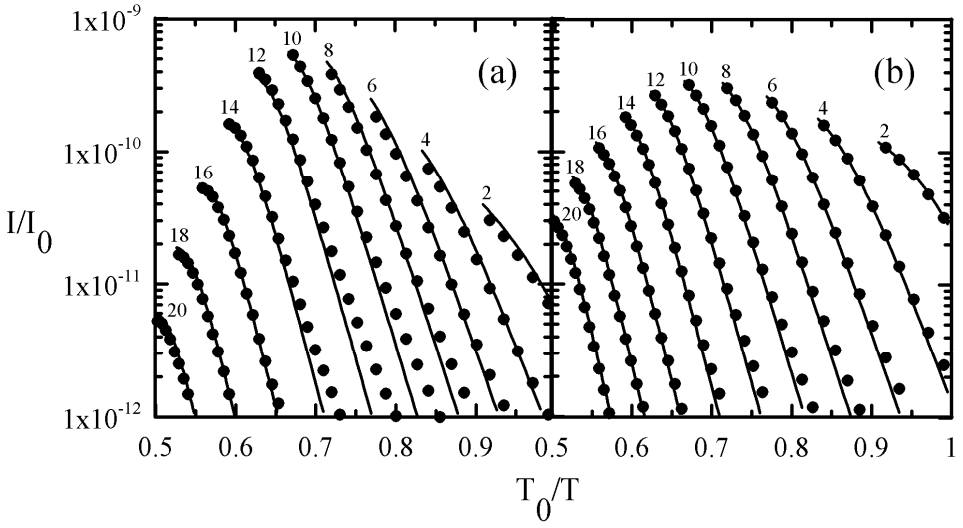

Fig. 3. Normalized TSCRP curves, corresponding to the monomolecular recombinetion and the exponential trap distribution. The parameters: $\tau_t\beta/T_0 = 10^{-12}$ (*a*), 10^{-11} (*b*); $\tau_R\beta/T_0 = 3\times10^{-10}$; $\nu_0 T_0/\beta = 10^{15}$; $\varepsilon_t^0/kT_0 = 30$; $T_C/T_0 = 3$ (*a*), 5 (*b*)

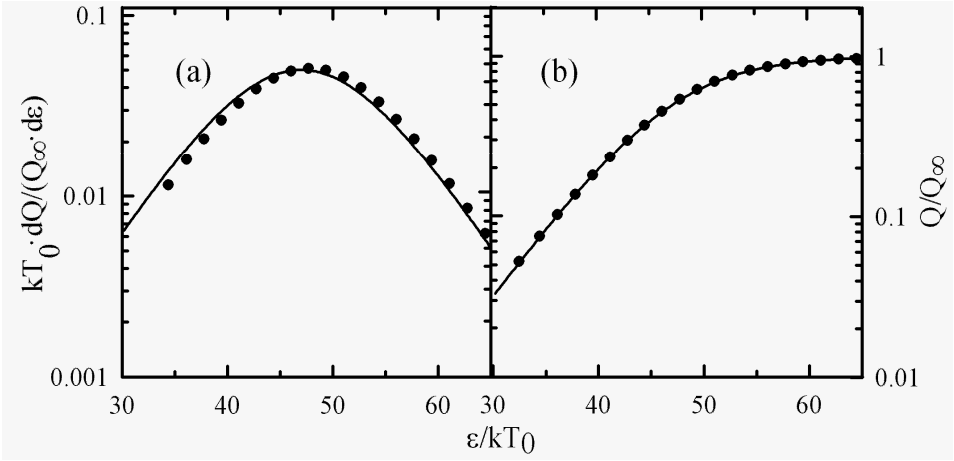

Fig. 4. Dependence of the energy derivative of collected charge (a) and of the collected charge (b) on the demarcation energy for the TSCRP at monomolecular recombination. The calculation parameters are as in Fig. 3, *b*

$dQ(\varepsilon)/d\varepsilon$ differ significantly from the course of trap density $N_t(\varepsilon)$, i.e., the relationship (36) does not hold in entire energy region.

Fig. 9 presents the comparison of the trap distributions (points), determined from the computed numerically TSCs by the B method, with the input distributions (continuous lines). In calculations the exact values of demarcation energy ε_m (cf. Fig. 2) have been used. For the present results, the relative error in determination of trap density is significant, particularly in the lower energy region and for smaller values of the T_C/T_0

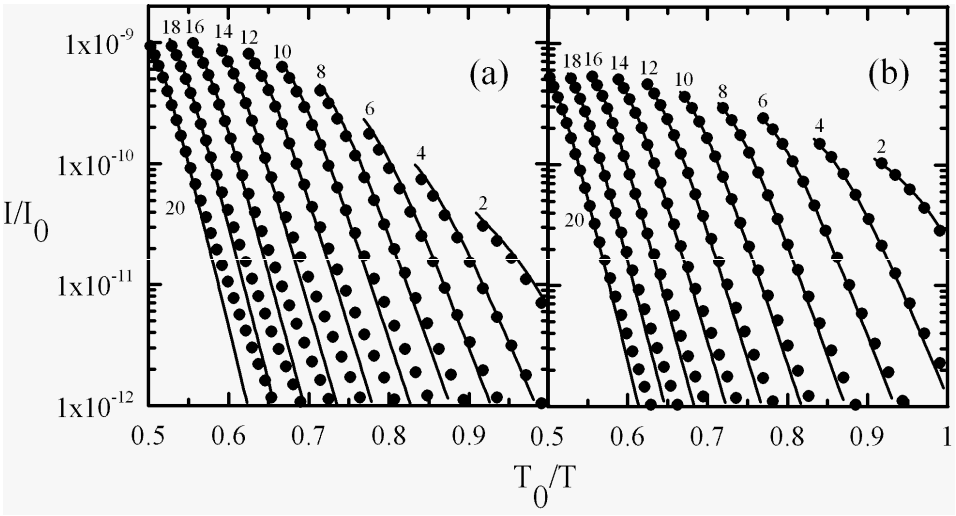

Fig. 5. Normalized TSCRP curves, corresponding to the bimolecular recombination and the exponential trap distribution. $\tau_t\beta/T_0 = 10^{-12}$ (*a*), 10^{-11} (*b*); $C_R n_0 T_0/\beta = 5\times10^9$; other parameters as in Fig. 3

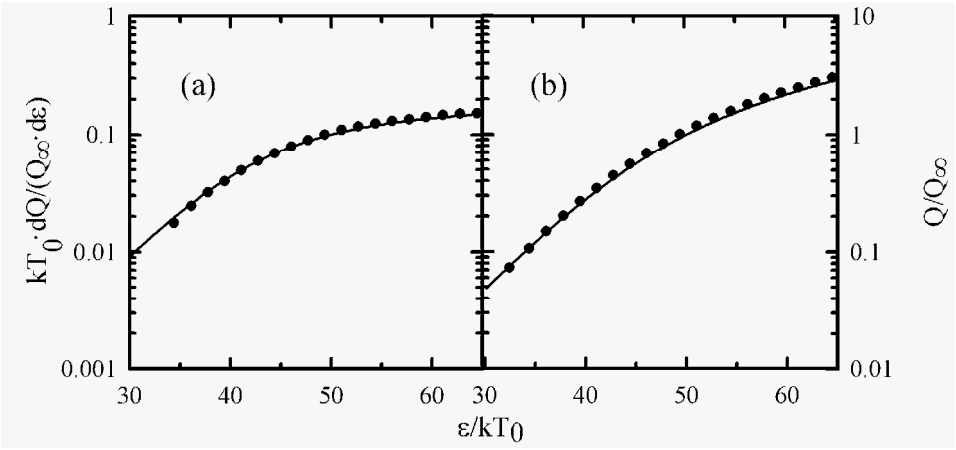

Fig. 6. Dependence of the energy derivative of collected charge (*a*) and of the collected charge (*b*) on the demarcation energy for the TSCRP at bimolecular recombination. The calculation parameters are as in Fig. 5, *b*

ratio, and amounts to 300%. However, since the trap densities vary with energy over several orders of magnitude, such accuracy seems to be acceptable. In practice, the error could be somewhat larger, due to uncertainty in determination of the demarcation energy.

In conclusion, the proposed methods of analysis of TSCs measured at step sample heating have reasonable accuracy and could be useful in experimental practice. The

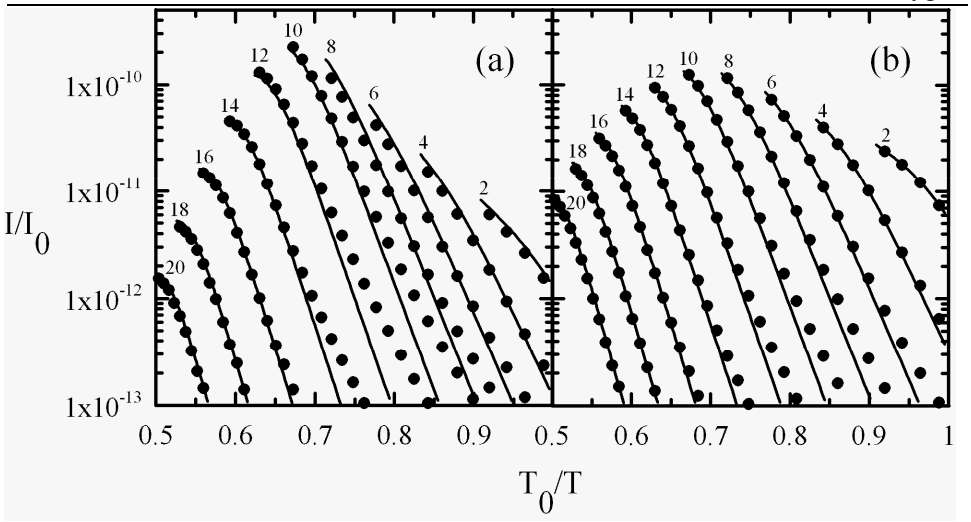

Fig. 7. Normalized TSCTP curves, corresponding to the exponential trap distribution. $\tau_t\beta/T_0 = 2\times10^{-13}$ (*a*), 2×10^{-12} (*b*); $\tau_0\beta/T_0 = 10^{-10}$; other parameters as in Fig. 3

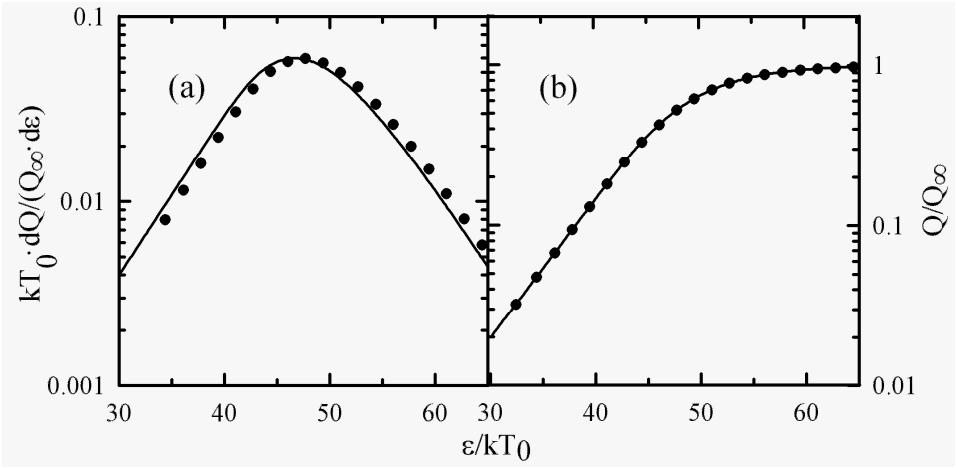

Fig. 8. Dependence of the energy derivative of collected charge (*a*) and of the collected charge (b) on the demarcation energy for the TSCTP. The calculation parameters are as in Fig. 7, *b*

analogous methods should also apply to the TSCs registered at fractional heating. This will be the subject of future paper.

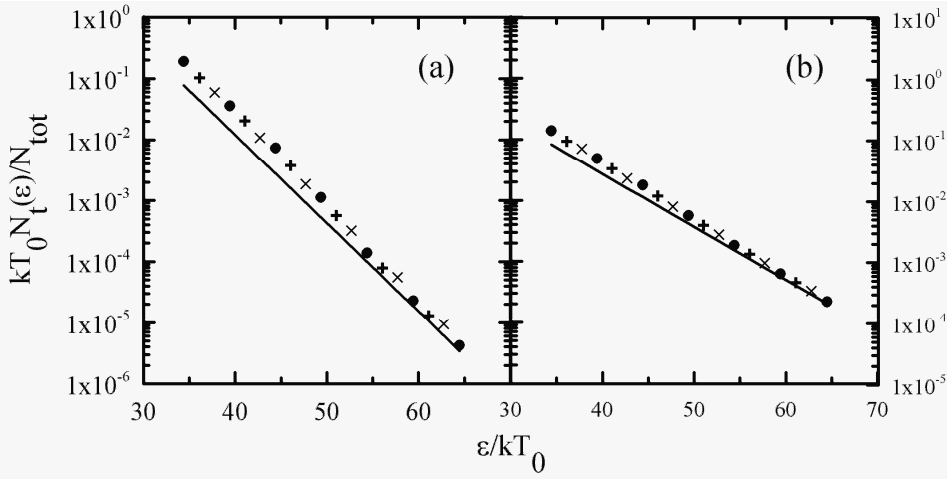

Fig. 9. The output trap distributions, calculated from the TSCRPs at monomolecular (+) and bimolecular (×) recombination and TSCTPs (•), compared with the input distributions (solid lines). The parameters for the plots (*a*) and (*b*) are the same as for the corresponding plots in Figs. 3, 5, and 7

The function $y=F_1(x)$ is the inverse of the function (23). For $y>>1$ the exponential function in Eq. (23) may be omitted, which gives

$$x \cong 1/y, \tag{A1}$$

and

$$F_1(x) \cong 1/x, \quad x << 1. \tag{A2}$$

For $y<<1$ the exponential function in Eq. (23) can be approximated by three initial terms of its expansion into power series, which results in

$$x \cong 1 - y/2, \tag{A3}$$

and

$$F_1(x) \cong 2(1-x), \quad x \cong 1. \tag{A4}$$

The $F_2(x)$ function is defined by Eq. (27). From Eqs. (A2) and (A4) it follows that

$$F_2(x) \cong 1/x^2, \quad x << 1, \tag{A5}$$

$$F_2(x) \cong 2, \quad x \cong 1. \tag{A6}$$

The plots of the $F_1(...)$ and $F_2(...)$ functions are shown in Fig. A1.

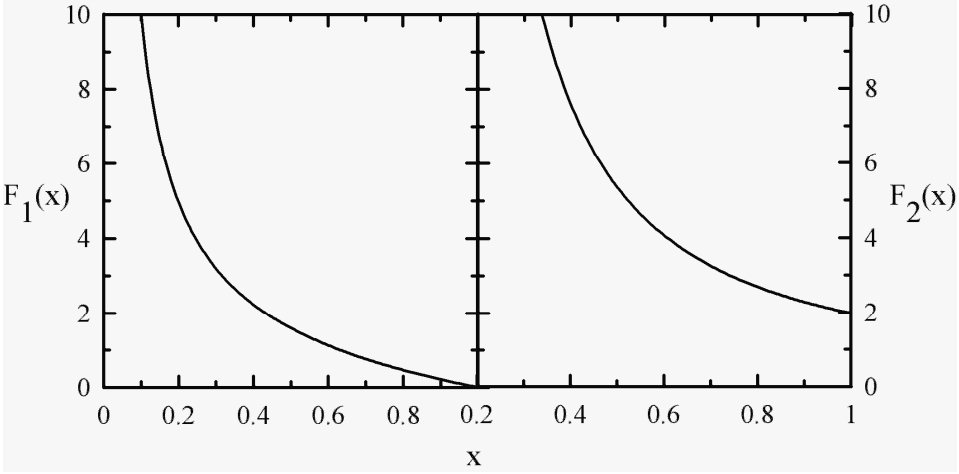

Fig. A1. Plots of the functions $F_1(x)$ and $F_2(x)$

1. *Fritzsche H., Ibaraki N.* Thermostimulated conductivity in amorphous materials // Philos. Mag. B. 1985. Vol. 52. N 3. P. 299–311.
2. *Misra D.S., Singh V.A., Agarwal S.C.* Analysis of thermally stimulated currents in amorphous silicon // Phys. Rev. B. 1985. Vol. 32. N 6. P. 4052–4059.
3. *Valentin F., Vaillant F., Deneuville A.* Study of localized states in glow discharge *a*-Si:H from thermally stimulated currents // J. Non-Cryst. Solids. 1987. Vol. 97&98. PT.1. P. 583–586.
4. *Slovik J.H.* Transport of photogenerated carriers in poly N-vinylcarbazole // J. Appl. Phys. 1976. Vol. 47. N 7. P. 2982–2987.
5. *Głowacki I., Ulański J.* Simultaneous measurements of thermoluminescence and thermally stimulated currents in poly(N-vinylcarbazole)/polycarbonate blends // J. Appl. Phys. 1995. Vol. 78. N 2. P. 1019–1025.
6. *Werner A.G., Blochwitz J., Pfeiffer M., Leo K.* Field dependence of thermally stimulated currents in Alq_3 // J. Appl. Phys. 2000. Vol. 90. N 1. P. 123–125.
7. *von Malm N., Schmechel R., von Seggern H.* Distribution of occupied states in doped organic hole transport materials // Synth. Metals. 2002. Vol.126. N 1. P. 87–95.
8. *Steiger J., Schmechel R., von Seggern H.* Energetic trap distributions in organic semiconductors // Synth. Metals. 2002. Vol. 129. N 1. P. 1–7.
9. *Gorokhovatskii Yu., Bordovskii G.* Thermally Activational Current Spectroscopy of High-resistance Semiconductors and Dielectrics. Moscow, 1991. 243 p.
10. *Plans J., Zieliński M., Kryszewski M.* Theory of thermally stimulated current transport peak // Phys. Rev. B. 1981. Vol. 23. N 12. P. 6557–6569.

11. *Tomaszewicz W.* Influence of sample heating mode on thermally stimulated currents in amorphous solids // Proc. VIIth Int. Seminar on Physics and Chemistry of Solids. Częstochowa, June 10-13, Poland, 2001. P. 67–77.
12. *Tomaszewicz W.* Thermally stimulated carrier due to stepwise sample heating // Macromolecular Symp. 2004. Vol. 212. N 7. P. 363–368.
13. *Tomaszewicz W.* Thermally stimulated currents in amorphous solids due to complex heating regimes // J. Non-Cryst. Solids. Accepted for publication.
14. *Gobrecht H., Hofmann D.* Spectroscopy of traps by fractional glow technique // J. Phys. Chem. Solids. 1966. Vol. 27. N 3. P. 509–522.
15. *Tomaszewicz W., Rybicki J., Grygiel P.* On thermally stimulated currents under dispersive transport regime // J. Non-Cryst. Solids. 1997. Vol. 221. P. 84–88.
16. *Tomaszewicz W.* Thermally stimulated currents due to multiple-trapping carrier transport: II. Dispersive transport // J. Phys.: Condens. Matter. 1992. Vol. 4. P. 3985–4002.
17. *Tomaszewicz W.* Thermally stimulated currents due to multiple-trapping carrier transport: I. Gaussian transport // J. Phys.: Condens. Matter. 1992. Vol. 4. P. 3967–3984.
18. *Tomaszewicz W., Grygiel P.* On thermally stimulated currents under quasi-equilibrium transport regime // Proc. SPIE. 2000. Vol. 37DP. P. 78–82.

ТЕРМОСТИМУЛЬОВАНІ СТРУМИ У НЕВПОРЯДКОВАНИХ ТВЕРДИХ ТІЛАХ, ЩО ВИНИКАЮТЬ ПІД ЧАС ПОКРОКОВОГО НАГРІВАННЯ

В. Томашевич, П. Григіель

Відділ явищ у фізиці і електроніці
Гданський технологічний університет
вул. Г.Нарутовіча 11/12, PL-80952 Гданськ, Республіка Польща

Теоретично досліджено термостимульовані струми (ТСС) в невпорядкованих твердих тілах, що виникають під час покрокового нагрівання. Розвинуто метод Гобрехта–Гофмана для випадку перезахоплення носіїв. Проаналізовано результати експериментальних вимірювань ТСС для зразків з компланарними електродами та електродами типу „сандвіч". З'ясовано, що головним чинником, який обмежує ТСС, є, відповідно, рекомбінація носіїв (моно- чи бімолекулярна) або їх нейтралізація на електроді. Для обох випадків отримано співвідношення, що дають змогу визначити енергетичний внесок пасток у разі посилення ТСС під час послідовних циклів нагрівання. Достовірність отриманих співвідношень оцінювали на підставі аналізу ТСС кривих, розрахованих для експоненційного внеску пасток.

Ключові слова: термостимульовані струми, покрокове нагрівання, захоплення носіїв, рекомбінація носіїв, багатопасткова модель, аморфні тіла.

Стаття надійшла до редколегії 29.05.2006
Прийнята до друку 26.02.2007